



Naturalis Repository

The pace of life for forest trees

Lalasia Bialic-Murphy, Robert M. McElderry, Adriane Esquivel-Muelbert [and others]

DOI:

<https://doi.org/10.1126/science.adk9616>

Downloaded from

[Naturalis Repository](#)

Article 25fa Dutch Copyright Act (DCA) - End User Rights

This publication is distributed under the terms of Article 25fa of the Dutch Copyright Act (Auteurswet) with consent from the author. Dutch law entitles the maker of a short scientific work funded either wholly or partially by Dutch public funds to make that work publicly available following a reasonable period after the work was first published, provided that reference is made to the source of the first publication of the work.

This publication is distributed under the Naturalis Biodiversity Center 'Taverne implementation' programme. In this programme, research output of Naturalis researchers and collection managers that complies with the legal requirements of Article 25fa of the Dutch Copyright Act is distributed online and free of barriers in the Naturalis institutional repository. Research output is distributed six months after its first online publication in the original published version and with proper attribution to the source of the original publication.

You are permitted to download and use the publication for personal purposes. All rights remain with the author(s) and copyrights owner(s) of this work. Any use of the publication other than authorized under this license or copyright law is prohibited.

If you believe that digital publication of certain material infringes any of your rights or (privacy) interests, please let the department of Collection Information know, stating your reasons. In case of a legitimate complaint, Collection Information will make the material inaccessible. Please contact us through email: collectie.informatie@naturalis.nl. We will contact you as soon as possible.

RESEARCH

TREE TRAITS

The pace of life for forest trees

Lasalia Bialic-Murphy^{1*}, Robert M. McDelderry^{1,2}, Adriane Esquivel-Muelbert³, Johan van den Hoogen¹, Pieter A. Zuidema⁴, Oliver L. Phillips⁵, Edmar Almeida de Oliveira⁶, Patricia Alvarez Loayza⁷, Esteban Alvarez-Davila⁸, Luciana F. Alves⁹, Vinicius Andrade Maia¹⁰, Simone Aparecida Vieira¹¹, Lidiany Carolina Arantes da Silva¹⁰, Alejandro Araujo-Murakami¹², Eric Arets¹³, Julien Astigarraga¹⁴, Fabrício Baccaro¹⁵, Timothy Baker⁵, Olaf Banki¹⁶, Jorcely Barroso¹⁷, Lilian Blanc¹⁸, Damien Bonal¹⁹, Frans Bongers²⁰, Kauane Maiara Bordin²¹, Roel Brienen⁵, Marcelo Brilhante de Medeiros²², José Luís Camargo²³, Felipe Carvalho Araújo¹⁰, Carolina V. Castilho²⁴, Wendeson Castro²⁵, Victor Chama Moscoso²⁶, James Comiskey^{27,28}, Flávia Costa²⁹, Sandra Cristina Müller²¹, Everton Cristo de Almeida³⁰, Antonio Carlos Lôla da Costa³¹, Vitor de Andrade Kamimura³², Fernanda de Oliveira¹⁰, Jhon del Aguila Pasquel^{33,34}, Géraldine Derroire³⁵, Kyle Dexter³⁶, Anthony Di Fiore^{37,38}, Louis Duchesne³⁹, Thaise Emílio⁴⁰†, Camila Laís Farrapo¹⁰, Sophie Fauset⁴¹, Frederick C. Draper⁴², Ted R. Feldpausch⁴³, Rafael Flora Ramos⁴⁴, Valeria Forni Martins^{45,21}, Marcelo Fragomeni Simon²², Miguel Gama Reis¹⁰, Angelo Gilberto Manzatto⁴⁶, Bruno Herault¹⁸, Rafael Herrera⁴⁷, Eurídice Honorio Coronado⁴⁸, Robert Howe⁴⁹, Isau Huamantupa-Chuquimaco⁵⁰, Walter Huaraca Huasco⁵¹, Katia Janaina Zanini²¹, Carlos Joly⁵², Timothy Killeen⁵³, Joice Klipel²¹, Susan G. Laurance⁵⁴, William F. Laurance⁵⁴, Marco Aurélio Leite Fontes¹⁰, Wilmar Lopez Oviedo⁵⁵, William E. Magnusson⁵⁶, Rubens Manoel dos Santos¹⁰, Jose Luis Marcelo Peña⁵⁷, Karla Maria Pedra de Abreu⁵⁸, Beatriz Marimon⁶, Ben Hur Marimon Junior⁶, Karina Melgaço⁵⁹, Omar Aurelio Melo Cruz⁵⁹, Casimiro Mendoza⁶⁰, Abel Monteagudo-Mendoza⁶¹, Paulo S. Morandi⁶, Fernanda Moreira Gianasi¹⁰, Henrique Nascimento⁶², Marcelo Nascimento⁶³, David Neill⁶⁴, Walter Palacios⁶⁵, Nadir C. Pallqui Camacho⁵, Guido Pardo⁶⁶, R. Toby Pennington^{67,68}, Maria Cristina Peñuela-Mora⁶⁹, Nigel C. A. Pitman⁷⁰, Lourens Poorter⁴, Adriana Prieto Cruz⁷¹, Hirma Ramírez-Angulo⁷², Simone Matias Reis^{73,6}, Zorayda Restrepo Correa⁷⁴, Carlos Reynel Rodriguez⁷⁵, Agustín Rudas Lleras⁷⁶, Flavio A. M. Santos⁵², Rodrigo Scarton Bergamin⁷⁷, Juliana Schietti¹⁵, Gustavo Schwartz⁷⁸, Julio Serrano⁷⁹, André Maciel Silva-Sene¹⁰, Marcos Silveira⁸⁰, Juliana Stropp⁸¹, Hans ter Steege^{16,82}, John Terborgh^{83,54}, Mathias W. Tobler⁸⁴, Luis Valenzuela Gamarra⁵³, Peter J. van der Meer⁸⁵, Geertje van der Heijden⁸⁶, Rodolfo Vasquez⁸⁷, Emilio Vilanova⁸⁸, Vincent Antoine Vos⁸⁹, Amy Wolf⁹⁰, Christopher W. Woodall⁹¹, Virginia Wortel⁹², Joeri A. Zwerts⁹³, Thomas A. M. Pugh^{94,3}, Thomas W. Crowther¹

Tree growth and longevity trade-offs fundamentally shape the terrestrial carbon balance. Yet, we lack a unified understanding of how such trade-offs vary across the world's forests. By mapping life history traits for a wide range of species across the Americas, we reveal considerable variation in life expectancies from 10 centimeters in diameter (ranging from 1.3 to 3195 years) and show that the pace of life for trees can be accurately classified into four demographic functional types. We found emergent patterns in the strength of trade-offs between growth and longevity across a temperature gradient. Furthermore, we show that the diversity of life history traits varies predictably across forest biomes, giving rise to a positive relationship between trait diversity and productivity. Our pan-latitudinal assessment provides new insights into the demographic mechanisms that govern the carbon turnover rate across forest biomes.

The cumulative energetic investment in survival and growth from one year to the next ultimately determines an organism's overarching pace of life, including the time it takes to grow to its maximal size and its life expectancy (1, 2). This fundamental relationship between energetic investments, developmental schedules, and longevity has been extensively studied for animals, showing that high resource allocation toward growth is inversely related to life expectancy and maximal body mass (3, 4). Trees are also assumed to retain tightly coupled relationships between growth strategies, life expectancies, and maximal sizes (Fig. 1A) (5), which determine the dynamics and structure of global forests. Yet, although these life history differences fundamentally regulate how fast carbon is sequestered in different regions of the vegetation carbon pool (6–8), we still lack a unified understand-

ing of the range of tree life history strategies that exist across global forests.

It is widely accepted that tree life history strategies should align along a primary axis of variation in their pace of life, ranging from fast-growing, short-lived species to slow-growing, long-lived species (i.e., fast-slow continuum and r/K selection theory) (Fig. 1A) (5). In this context, high energetic investment of finite resources toward fast growth is expected to come at the cost of reduced survival, which ultimately determines a species' life expectancy and maximal size (Fig. 1A) (9–11). Thus, it is expected that abiotic constraints (e.g., soil nutrients, water, and temperature) should strongly shape the pace of life for trees, giving rise to predictable variation in the strength of life history trade-offs across biogeographic gradients (Fig. 1B) (12). So far, however, the only empirical tests of these trade-offs come from

tree ring data and local-scale studies from tropical ecosystems and have produced mixed results (2, 12–14).

One potential challenge that can obscure predictable patterns in the pace of life for trees is that it is not only the traits that are expected to vary across environmental gradients but also the diversity of those traits. For example, strong biotic competition across tropical forests is thought to have led to high demographic niche differentiation (i.e., high demographic diversity; Fig. 1C, upper right). By contrast, resource limitations in harsh cold and dry regions are assumed to have restricted the species pool to predominantly slow-growing, long-lived species (Fig. 1C, lower left). Yet, these suppositions lack empirical evidence to support them because the extreme longevity of trees (which can live for thousands of years) has precluded our capacity to quantify the strength of tree life history trade-offs across a wide range of species, let alone characterize the diversity of life history traits across biogeographic gradients.

In this study, we used the largest dataset of dynamic tree information to date and used age-from-stage methods to calculate the mean life expectancy and maximal life span for a wide range of trees across the Americas (15–17), spanning a latitudinal gradient from Northern Canada to Southern Brazil. This includes long-term records from an international network of researchers, including members of the Global Forest Dynamics, ForestPlots.net (18, 19), and ForestGeo (20–22) networks and the United States and Canadian forest inventory programs (23–25). To balance this dataset across our biogeographic gradient, we randomly subsampled the North American plots to equal the number of point observations in Central and South America [see supplementary materials (SM), materials and methods], resulting in 3.2 million distinct tree measurements for 1127 species (i.e., tree size and status). Our big-data approach allowed us to test for the expectation that trees align along the fast-slow continuum (Fig. 1A, H1) and to quantify whether tree growth–longevity–stature relationships covary across soil, water, and temperature gradients (Fig. 1B, H2). Apart from species with low occurrences (<100 observations; see SM, materials and methods), our systematic sampling allowed us to test for the expectation that the range of life history strategies occupied by species (i.e., demographic trait diversity) varies predictably across broadscale biogeographic gradients, with harsh cold regions in the Northern Hemisphere restricting trees to a smaller pool of predominantly slow-growing, long-lived species (Fig. 1C, H3). On the basis of the well-established diversity–productivity relationship, we also expected demographic trait diversity to be positively associated with ecosystem productivity (Fig. 1C, H3).

To quantify tree growth, longevity, and stature for a wide range of species across biogeographic gradients and test our three core hypotheses, we

first grouped the stem-level tree data into equally sized hexagon grids (size ~250,000 km²) and developed species-specific survival- and growth-

generalized linear mixed-effects models that included tree diameter at breast height (dbh) at the first census interval as a predictor variable

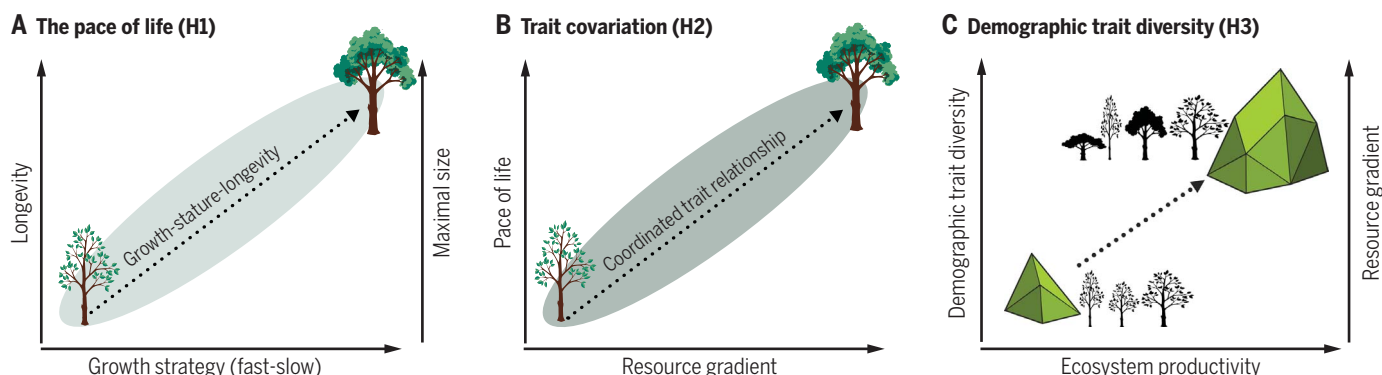


Fig. 1. Conceptual diagram of our core aims and associated hypotheses.

(A) The expectation is that trees should align along the fast-slow continuum, with fast-growing, short-lived species on one end of the spectrum and slow-growing, long-lived species on the other end (H1). (B) Life history trait relationships should be phylogenetically conserved and should covary across biogeographic gradients, leading to

more conservative life history strategies in low-resource environments (low soil and nutrient environments and colder temperatures) (H2). (C) Lastly, we expect the range of tree life history strategies (i.e., convex-hull volume in life history trait space that is occupied by species) to vary predictably across biogeographic gradients, with demographic trait diversity being positively associated with ecosystem productivity (H3).

- ¹Institute of Integrative Biology, ETH Zurich (Swiss Federal Institute of Technology), 8092 Zurich, Switzerland. ²Forest Health and Biotic Interactions, Swiss Federal Research Institute WSL, 8903 Birmensdorf, Switzerland. ³Birmingham Institute of Forest Research (BIFoR), University of Birmingham, Birmingham, UK. ⁴Forest Ecology and Forest Management Group, Wageningen University & Research, Wageningen, Netherlands. ⁵School of Geography, University of Leeds, Leeds, UK. ⁶Universidade do Estado de Mato Grosso (Unemat) - Pós-Graduação em Ecologia e Conservação, Nova Xavantina-MT, Brazil. ⁷Nicholas School of the Environment, Duke University, Durham, NC 27710, USA. ⁸Escuela de Ciencias Agrícola, Universidad Nacional Abierta y a Distancia de Colombia, Colombia. ⁹Center for Tropical Research, Institute of the Environment and Sustainability, University of California, Los Angeles, Los Angeles, CA 90095, USA. ¹⁰Universidade Federal de Lavras, Lavras, Brazil. ¹¹Universidade Estadual de Campinas, Campinas, Brazil. ¹²Museo de Historia Natural Noel Kempff Mercado, Universidad Autónoma Gabriel René Moreno, Santa Cruz, Bolivia. ¹³Wageningen Environmental Research, Wageningen University & Research, Wageningen, Netherlands. ¹⁴Universidad de Alcalá, Department of Life Sciences, Forest Ecology and Restoration Group (FORECO), Alcalá de Henares, Spain. ¹⁵Universidade Federal do Amazonas, Manaus, Brazil. ¹⁶Naturalis Biodiversity Center, Leiden, Netherlands. ¹⁷Laboratório de Ciências Florestais, Universidade Federal do Acre, Campus de Cruzeiro do Sul, Acre, Brazil. ¹⁸Forêts et Sociétés, Université Montpellier, CIRAD, Montpellier, France. ¹⁹Université de Lorraine, AgroParisTech, INRAE, UMR Silva, 54000 Nancy, France. ²⁰Department of Environmental Sciences, Wageningen University & Research, Wageningen, Netherlands. ²¹Plant Ecology Lab, Ecology Department, Universidade Federal do Rio Grande do Sul, Porto Alegre, Brazil. ²²Embrapa Genetic Resources and Biotechnology, Brasília, Brazil. ²³Biological Dynamics of Forest Project - National Institute for Amazonian Research (BDFFP-INPA), Manaus, Brazil. ²⁴Embrapa Roraima, Boa Vista, Roraima, Brazil. ²⁵Centro de Ciências Biológicas e da Natureza, Universidade Federal do Acre, Rio Branco, Acre, Brazil. ²⁶Universidad Nacional de San Antonio Abad del Cusco, Cusco, Peru. ²⁷Inventory and Monitoring Program, National Park Service, Fort Collins, CO 80525, USA. ²⁸Smithsonian Institution, Washington, DC 20024, USA. ²⁹Coordenação de Pesquisas em Biodiversidade, Instituto Nacional de Pesquisas da Amazônia, CEP 69067-375, Manaus, Brazil. ³⁰Universidade Federal do Oeste do Pará (UFOPA), Instituto de Biodiversidade e Florestas (IBEF), Santarém, Pará, Brazil. ³¹Universidade Federal do Pará - Instituto de Geociências, Belém Pará, Brazil. ³²Instituto Tecnológico Vale (ITV), Belém, Pará, Brazil. ³³Instituto de Investigaciones de la Amazonia Peruana, Iquitos, Peru. ³⁴Universidad Nacional de la Amazonia Peruana, Iquitos, Peru. ³⁵Cirad, UMR EcoFoG (AgroParisTech, CNRS, INRAE, Université des Antilles, Université de la Guyane), Campus Agronomique, Kourou, French Guiana. ³⁶School of GeoSciences, University of Edinburgh, Royal Botanic Garden Edinburgh, Edinburgh, UK. ³⁷Primate Molecular Ecology and Evolution Laboratory and Department of Anthropology, The University of Texas at Austin, Austin, TX 78712 USA. ³⁸Tipitini Biodiversity Station, College of Biological and Environmental Sciences, Universidad San Francisco de Quito, Cumbay, Ecuador. ³⁹Direction de la Recherche Forestière, Ministère des Ressources Naturelles et des Forêts du Québec, Québec City, QC G1P 3W8, Canada. ⁴⁰Programa Nacional de Pós-Doutorado (PNPD), Programa de Pós-Graduação em Ecologia, Instituto de Biologia, Universidade de Campinas (UNICAMP), Campinas, Brazil. ⁴¹School of Geography, Earth and Environmental Sciences, University of Plymouth, Plymouth, UK. ⁴²School of Environmental Sciences, University of Liverpool, Liverpool, UK. ⁴³Geography, Faculty of Science, Environment and Economy, University of Exeter, Exeter, UK. ⁴⁴Biology Institute, University of Campinas, 13083-862, Campinas, SP, Brazil. ⁴⁵Department of Natural Sciences, Mathematics, and Education, Centre for Agrarian Sciences, Universidade Federal de São Carlos (UFSCar), Araras, SP, Brazil. ⁴⁶Federal University of Rondônia (Unir-Porto Velho, RO), Brazil. ⁴⁷Instituto Venezolano de Investigaciones Científicas (VIC), Miranda, Venezuela. ⁴⁸School of Geography and Sustainable Development, University of St Andrews, St Andrews, UK. ⁴⁹Cofrin Center for Biodiversity, University of Wisconsin-Green Bay, Green Bay, WI 54311, USA. ⁵⁰Herbario "Alwyn Gentry" (HAG), Universidad Nacional Amazónica de Madre de Dios (UNAMAD), Puerto Maldonado, Madre de Dios, Perú. ⁵¹Environmental Change Institute, School of Geography and the Environment, University of Oxford, Oxford, UK. ⁵²Plant Biology Department, Biology Institute, University of Campinas, Campinas, SP, Brazil. ⁵³Missouri Botanical Garden, St. Louis, MO 63110, USA. ⁵⁴Centre for Tropical Environmental and Sustainability Science, College of Science and Engineering, James Cook University, Cairns, Australia. ⁵⁵Smurfit Kappa Colombia, Yumbo, Valle del Cauca, Colombia. ⁵⁶Instituto Nacional de Pesquisas da Amazônia, Manaus, Brazil. ⁵⁷Universidad Nacional de Jaén, Laboratory of Vascular Plants and ISV Herbarium, San Ignacio, Peru. ⁵⁸Federal Institute of Espírito Santo, Campus de Alegre, Alegre, ES, Brazil. ⁵⁹Universidad del Tolima, Ibagué, Colombia. ⁶⁰Universidad Mayor de San Simón, Cochabamba, Bolivia. ⁶¹Universidad Nacional de San Antonio Abad del Cusco, Jardín Botánico de Missouri, Cusco, Peru. ⁶²Biodiversity Department, Instituto Nacional de Pesquisas da Amazônia, Manaus, Brazil. ⁶³Laboratório de Ciências Ambientais, CBB, Universidade Estadual do Norte Fluminense Darcy Ribeiro, Campos dos Goytacazes, RJ, Brazil. ⁶⁴Universidad Estatal Amazonica, Puyo, Pastaza, Ecuador. ⁶⁵Instituto Nacional de Biodiversidad, INABIO, Quito, Ecuador. ⁶⁶Facultad de Ciencias Forestales, Universidad Autónoma del Beni José Ballivián, Riberalta, Beni, Bolivia. ⁶⁷Department of Geography, University of Exeter, UK. ⁶⁸Royal Botanic Garden, Edinburgh, UK. ⁶⁹Universidad Regional Amazónica Ikiam, Tena, Ecuador. ⁷⁰Collections, Conservation & Research, Field Museum of Natural History, Chicago, IL 60605, USA. ⁷¹ONF Andina, Bogotá, Colombia. ⁷²Universidad de Los Andes, Facultad de Ciencias Forestales y Ambientales, INDEFOR, Merida, Venezuela. ⁷³Ciências Biológicas e da Natureza, Universidade Federal do Acre, Rio Branco, Acre, Brazil. ⁷⁴Servicios Ecosistémicos y Cambio Climático, Corporación COL-TREE, Medellín, Colombia. ⁷⁵Universidad Nacional Agraria La Molina, Lima, Facultad de Ciencias Forestales, Lima, Peru. ⁷⁶Instituto de Ciencias Naturales, Universidad Nacional de Colombia, Bogotá, Colombia. ⁷⁷School of Geography, Earth and Environmental Science, University of Birmingham, UK. ⁷⁸Embrapa Eastern Amazon, 66095-903, Belém, PA, Brazil. ⁷⁹Universidad de Los Andes, Merida, Venezuela. ⁸⁰Laboratório de Botânica e Ecologia Vegetal, Centro de Ciências Biológicas e da Natureza, Universidade Federal do Acre, Acre, Brazil. ⁸¹Geography Department, Trier University, 54286 Trier, Germany. ⁸²Quantitative Biodiversity Dynamics, Department of Biology, Utrecht University, Utrecht, The Netherlands. ⁸³Florida Museum of Natural History, University of Florida-Gainesville, Gainesville, FL 32611, USA. ⁸⁴San Diego Zoo Wildlife Alliance, Escondido, CA 92027, USA. ⁸⁵Van Hall-Larenstein University of Applied Sciences Velp, Netherlands. ⁸⁶School of Geography, University of Nottingham, Nottingham NG7 2RD, UK. ⁸⁷Jardín Botánico de Missouri (JBM), Oxapampa, Pasco, Peru. ⁸⁸Wildlife Conservation Society (WCS), Bronx, NY 10460, USA. ⁸⁹Instituto de Investigaciones Forestales de la Amazonia, Universidad Autónoma del Beni José Ballivián, Riberalta, Beni, Bolivia. ⁹⁰University of Wisconsin-Green Bay, Department of Natural and Applied Sciences, Green Bay, WI 54311, USA. ⁹¹US Department of Agriculture, Forest Service, Research and Development, Durham, NH 03824, USA. ⁹²Department of Forest Management, Centre for Agricultural Research in Suriname, CELOS, Suriname. ⁹³Utrecht University, Utrecht, Netherlands. ⁹⁴Department of Physical Geography and Ecosystem Science, Lund University, Sweden.

*Corresponding author. Email: lalasia.bialicmurphy@usys.ethz.ch

†Present address: Center for Research on Biodiversity Dynamics and Climate Change (CBioClima), Institute of Biosciences, São Paulo State University (UNESP), Campus Rio Claro, SP, Brazil.

‡Present address: Institute of Ecology, Leuphana University of Lüneburg, Lüneburg, Germany.

§Present address: BeZero Carbon, London, UK.

and grid cell as a random effect (SM, materials and methods). We then used the survival and growth coefficients to fit size-dependent integral projection models (IPMs) and derive age-related traits from size-dependent probabilities for each species within each grid cell (SM, materials and methods) (15–17, 26–28). IPMs dynamically integrate size-dependent variability in survival and growth as a continuous process, which allowed us to use cross-sectional data over discrete time steps to make interspecific comparisons of how many years it takes trees to attain key milestones in their life cycle. We parameterized our IPMs using methods specifically developed for trees (27–29). Validations of IPM model outputs, relative to tree ring data, showed that this parameterization method can provide realistic estimates of tree age demographics (27).

We used our species-specific IPMs and age-from-stage methods to calculate several quantitative measures of growth, longevity, and stature. Specifically, we calculated the number of years it takes for trees to grow from 10 to 20 cm in diameter (fig. S2, path a.2) and to grow

from 10 cm to the 70th quantile of their size distribution (fig. S2, path a.1) (hereafter referred to as “growth strategies”). The 10-cm-diameter lower-bound threshold was chosen because it was the size at which point trees were consistently monitored across the forest networks, and the 70th quantile threshold was chosen because it reflects a mature size at which point trees have approached their ultimate position in the forest. We also calculated two quantitative measures of tree longevity, including their average remaining life expectancy from 10 cm in diameter and their maximal life-span age (95% cohort mortality from 10 cm) and a measure of maximal tree stature (size at maximal life-span age) (fig. S2, path b) (15–17). These mean estimates capture the pace of life for trees (growth, longevity, and stature) on the basis of observed climate conditions over the last century (derived from dynamical data collected between 1926 and 2014; see SM, materials and methods).

Our estimates of remaining life expectancy from 10 cm dbh range from 1.2 to 3195 years, with a mean value of 60 years in the tropics

and 95 years in the extratropics (Fig. 2A). This trend matches our theoretical expectation of broadscale tree life history diversification patterns (Fig. 1B) and confers with known tree longevity hotspots, in which the oldest recorded species occur in temperate conifer and boreal forests (12, 30). However, there was also considerable overlap in the range of tree life expectancies across biomes (figs. S3 and S4, and table S2) and wide variability in how longevity relates to tree growth strategies and maximal stature (Fig. 2B, figs. S3 and S4, and table S2). It is important to note that remaining life expectancy from 10 cm dbh is a species-level mean estimate (i.e., is conditional on surviving to 10 cm dbh). A low life expectancy, relative to the mean number of years it takes a species to grow from 10 to 20 cm dbh, does not imply that no individuals will reach 20 cm dbh. Instead, it implies that less than half of the individuals will survive to that size threshold.

Tree life history strategies do not strictly follow the fast-slow continuum (H1)

To test the expectation that trees align along the fast-slow continuum (Fig. 1A, H1), we first examined univariate trait correlations and found moderate support for trade-offs between tree growth, longevity, and stature (fig. S5). For example, the number of years it takes trees to grow from 10 to 20 cm in diameter was positively correlated to life expectancy [Pearson correlation coefficient (r) = 0.22] and maximal life-span age (Pearson's r = 0.21). Similarly, maximal tree size was positively related to life expectancy (Pearson's r = 0.41). The strength of these pairwise correlations also suggests that tree age demographics do not strictly follow a single axis of variation along the fast-slow continuum (i.e., the assumption that growth is tightly coupled and inversely related to longevity and maximal stature).

To examine the multidimensionality of tree age demographics (Fig. 1A, H1), we analyzed the variance-covariance matrix of tree growth, longevity, and stature using a principal components analysis (PCA). Highly correlated traits that captured redundant trait information were excluded from the PCA (fig. S5), resulting in the inclusion of tree growth strategies (i.e., growth from 10 to 20 cm dbh and the 70th quantile of their size distribution), life expectancy from 10 cm dbh, and maximal tree size (fig. S5). The first PC axis captured 46% of the life history trait variation and was heavily weighted by tree growth dynamics (i.e., years to 20 cm dbh and the 70th quantile size) (Fig. 2C). The PC loadings also showed that slow growth was correlated with high life expectancy and large maximal size (table S3). The second axis captured 28% of the trait variation. The directionality between the trait correlations flipped, whereby slow growth was negatively correlated to life expectancy and maximal size (table

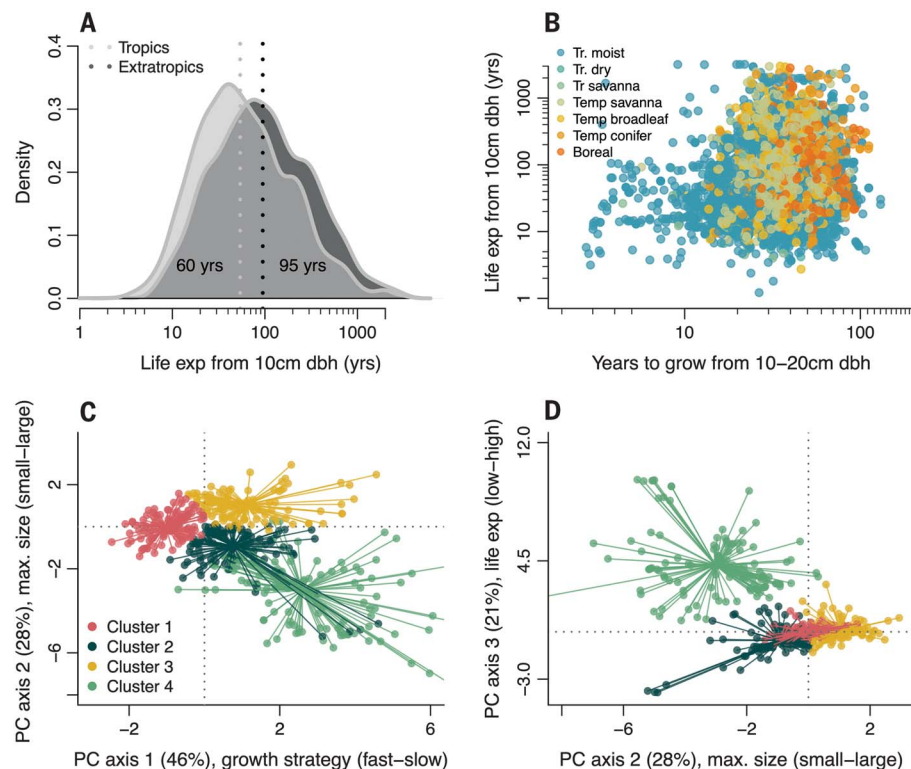


Fig. 2. Visual illustration of tree growth-longevity-stature relationships and core demographic functional types. The mean life expectancy is higher in the extratropics than in the tropics (A), with substantial variation between tree growth strategies and life expectancies (B) ($N = 6847$, i.e., species \times grid ID). The other trait relationships are represented in fig. S8. The core growth-longevity-stature functional types are presented in (C and D), which are determined using the k -means clustering algorithm of the life history trait principal components analysis (PCA) scores. PC weights and trait correlations are reported in table S3. The frequency density (A) and the life history traits (B) are scaled by the natural log. Data points are species-specific and are calculated using individual tree observations and size-dependent integral projection models (SM, materials and methods).

S3). The third axis was heavily weighted by tree life expectancy, with high life expectancy being positively related to slow growth but negatively related to tree maximal size (table S3). PCA analyses for tropical versus extratropical species retained consistent patterns in the directionality of the trait correlations among the PC axes (table S3), illustrating the modular and flexible nature of tree age demographics beyond the fast-slow continuum within and among the Northern and Southern hemispheres.

To further contextualize how the variation in tree age demographics among the PC axes shapes the overarching pace of life for trees, we used a *k*-means clustering algorithm to group species into core demographic functional types (SM, material and methods subsection 3, and fig. S6). Using this clustering algorithm, which reduces the within-group sum of squares, we found that fast-growing species aggregated into a single stature-longevity functional type (Fig. 2, C and D, cluster 1). Conversely, conservative slow-growing species formed three distinct clusters, including low, intermediate, and high stature-longevity functional types (Fig. 2, C and D, clusters 2 to 4). The fast-growing species cluster matches the theoretical expectation of ubiquitous resource limitations that constrain a species' ability to maintain high growth and high survival simultaneously, leading to low life expectancies and small maximal sizes (Fig. 2, C and D, cluster 1). Yet, the emergence of three distinct clusters for slow-growing species suggests that conservative trees are less constrained in their pace of life. At one end of these three conservative growth trait clusters were species with high life expectancies but small maximal sizes (Fig. 2, C and D, cluster 4), and at the other end were species with low life expectancies but large maximal sizes (Fig. 2, C and D, cluster 3). Clustering analyses for tropical versus extratropical species indicate that the tropics retain the full range of demographic functional types (fig. S7, four distinct clusters). Conversely, the extratropical species group into two to three demographic functional types of predominantly slow-growing conservative clusters (fig. S7, two to three distinct clusters). Together, these results provide key insight into the core groups of demographic functional types that shape the structural complexity and dynamics of tropical versus extratropical forests.

Our broadscale assessment of growth-longevity-stature relationships for a wide range of species across the Americas is consistent with trends derived from tropical forest plots, which found that survival and growth rates over discrete size ranges differed substantially among species and diminished as trees attained larger sizes (31–37). Similarly, although tree-ring data showed that annual growth rates were negatively correlated with observed maximal ages (12), there was more variation in observed maximal ages for species with fast

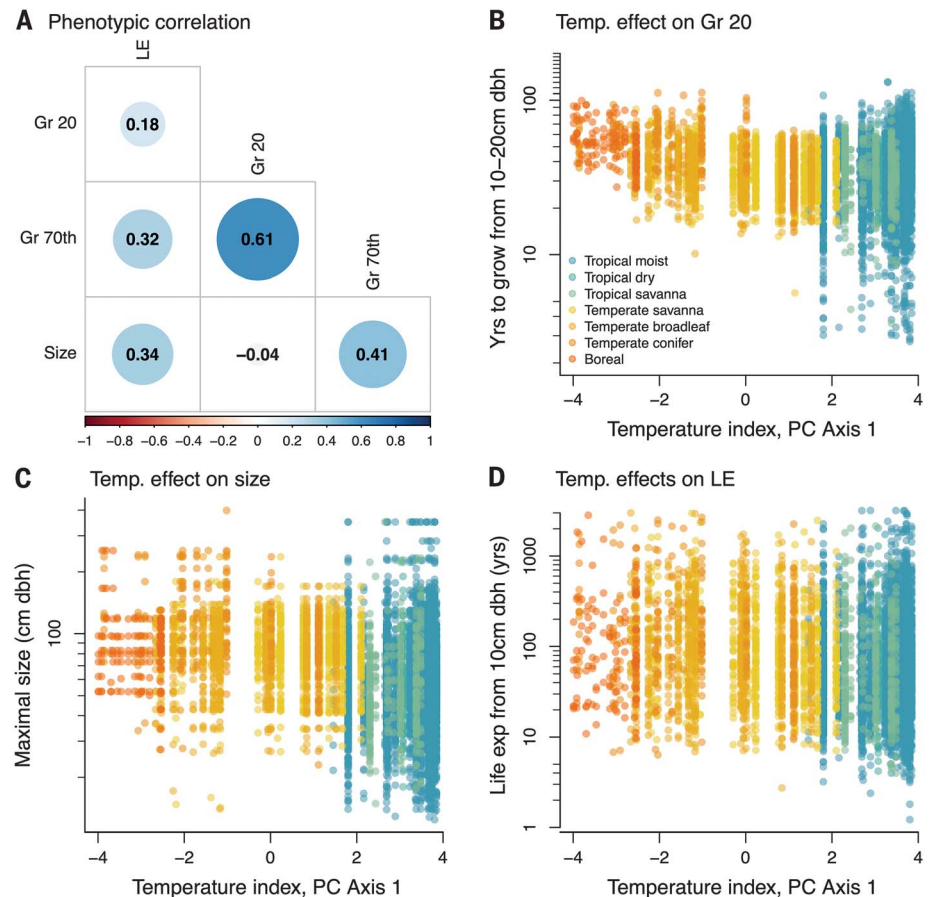


Fig. 3. Tree life history traits across our temperature index. (PC axis 1; for a comprehensive list of temperature variables, see SM, materials and methods). **(A)** Overall, we found low phenotypic correlations (variance-covariance of standardized traits) among tree growth, longevity, and stature across our biogeographic indexes, suggesting that there is weak support for coordinated trade-offs over evolutionary time (i.e., organismal function that supports conservative growth does not necessarily trade off with organismal function needed to maintain high longevity). **(B to D)** We also find a strong effect of temperature on tree life history traits, with little additional variation explained by soil or precipitation (figs. S12 and S13 and table S5). The temperature gradient is derived from a PCA of nine temperature variables and represents a gradient from intermediate temperatures in the tropical moist forest of the Southern Hemisphere to colder temperatures in the boreal north (from left to right of the x axis). The y axes are scaled by the natural log and the x axes are scaled to a mean of zero and a SD of 1. Data points are species-specific and are calculated using individual tree observations to fit size-based integral projection models for each species within each grid cell ID (total of 1127 species and 6847 trait values) (SM, materials and methods). Model coefficients of the multiresponse Bayesian model are reported in fig. S12 and table S5.

versus slow growth (12, 14). Together, these emergent patterns illustrate the modular and flexible nature of trees that extend beyond the fast-slow continuum (Fig. 2, C and D, and figs. S3 and S4) and highlight the tremendous variation in tree life expectancies across forest biomes (Fig. 2A and figs. S3 and S4), with some of the oldest living species having a remaining life expectancy >2000 years (such as *Tsuga heterophylla* and *Sequoia sempervirens*).

Building on these foundational insights from predominantly tropical ecosystems, our results provide a novel perspective that contributes to our fundamental understanding of tree age demographics. By converting survival and growth rates over species life cycles to age-based traits,

our results provide insight into the time it takes trees to reach their ultimate positions in the forest and their mean age at death (e.g., life expectancy). This allowed us to quantify the pace of life for a wide range of species across the Americas and identify the core demographic functional types more directly linked to carbon turnover. The emergence of the slow-growth short-life span functional trait cluster is in line with previous research from tropical forests, which showed that some short-stature trees had slow growth and low survival (31, 32, 34, 38). This emergent trend may be an indication of maladapted species or a mediated effect of environmental disturbance (10, 32, 33). Conversely, it could be the result of energetic investments in

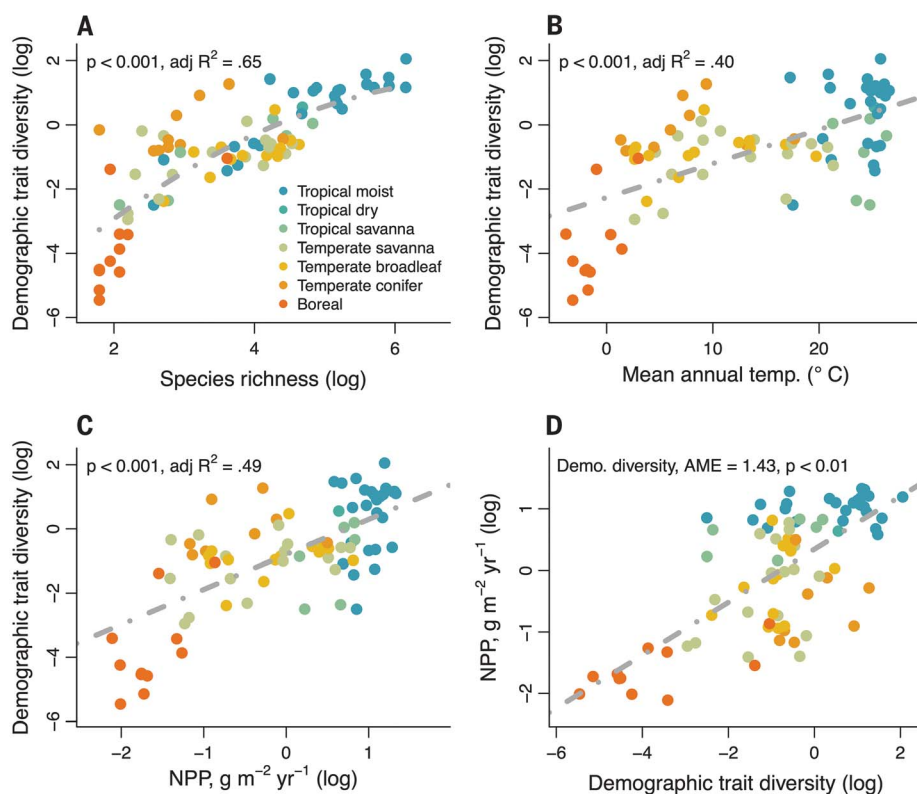


Fig. 4. The relationship between the demographic trait diversity of forests and ecosystem productivity (H3). We find that the demographic trait diversity is positively related to species richness (A), with increasing demographic trait diversity (i.e., convex-hull volume in life history trait space that is occupied by species) across a mean annual temperature gradient (B). In line with two nonmutually exclusive hypotheses in evolutionary biology and functional ecology, we find a positive association between demographic trait diversity and aboveground net primary productivity (NPP) (C and D). It is important to note that NPP was based on remotely sensed estimates and that these analyses do not establish causality in the directionality of this relationship [(C) and (D)]. The fully parameterized model in (D) includes the demographic trait diversity and mean annual temperature. Demographic trait diversity and NPP were scaled to a mean of zero and a SD of 1. Average marginal effects (AME) represent the response per unit increase for each predictor variable.

reproduction over species' life spans (net reproductive rate) that we were not able to capture in our analysis (5, 11, 31, 34). Regardless of the mechanisms, our findings provide a novel perspective on the multidimensionality of tree age demographics for a wide range of phylogenetic and geographical groups. Furthermore, our finding of emergent differences in the number of demographic functional types in the tropics versus extratropics offers novel insight into the mechanisms that shape the dynamics and structure of forests across the Americas.

Weak coordination in the strength of life history trade-offs across biogeographic gradients (H2)

To test for emergent patterns in the strength of tree life history trade-offs across biogeographic gradients (Fig. 1B, H2), we fit a multiresponse Bayesian generalized mixed-effects model that included the first PC axis for each of three comprehensive sets of variables related to soil, temperature, and precipitation as fixed effects and the phylogenetic relatedness as a random

effect (SM, materials and methods; table S4; and figs. S6 to S8) (39). These abiotic indexes were selected because they are known to strongly regulate photosynthetic capacity and plant growth and are commonly assumed to induce life history trade-offs. This approach allowed us to test for covariation in life history trait responses across soil, temperature, and precipitation indexes and control for the effects of phylogenetic ancestry (40). These soil, temperature, and precipitation variables were based on mean conditions from 1997 to 2013 (SM, materials and methods, and table S4), which overlap with the time window that our dynamical tree data were collected. The expectation is that tree life history trade-offs are shaped by the shared influence of abiotic factors and phylogenetic constraints, with colder temperatures and lower resource availability pushing species toward the conservative end of the life history trait spectrum (Fig. 1B, H2).

Our results show that there is a strong relationship between temperature and tree life

history traits, with colder temperatures being associated with conservative growth [$\beta = -0.02$, confidence interval (CI) = $(-0.03, -0.01)$] and high life expectancies [$\beta = -0.07$, CI = $(-0.05, -0.08)$] (Fig. 3 and fig. S12). Conversely, our precipitation and soil indices had a weak effect on life history traits (fig. S12 and table S5). Consistent with Amazon research (41), we found that tree life history traits were phylogenetically conserved (Pagel's λ ranging from 0.88 to 0.99; fig. S14 and table S6). Yet, we also found low phenotypic correlations among our life history traits, indicating that the strength of trade-offs between tree growth, longevity, and stature do not strongly covary across biogeographic gradients (Fig. 1B, H2). For example, the phenotypic correlation between the number of years it takes trees to grow to 20 cm dbh and their life expectancy from 10 cm dbh was 0.18 (Fig. 3A). Together, these results show that, although tree life history traits are phylogenetically conserved [Δ deviance information criterion (DIC) null model versus phylogenetic model = 76832], growth-longevity-stature relationships are not driven by genetic linkages or shared selective pressures that act on both traits independently over evolutionary time across broadscale resource gradients (table S6) (42).

Although our results offer the most comprehensive assessment of tree age demographics across broadscale resource gradients, it is important to note the data gap in the subtropics (i.e., across Mexico and northern Central America; fig. S1). This data gap could help explain the noticeable difference in the range of life history trait strategies between the North American temperate forests (low trait variation) and South American tropical forests (high trait variation) (Fig. 3, B to D, and fig. S1). This data gap highlights the need for increased sampling efforts in these understudied regions of the world and should be a priority of future research and funding.

Our findings are in line with trade-offs between physiological and morphological plant features linked to individual fitness and life history evolution, one reflecting leaf economic variables related to photosynthetic activity and growth potential and the other associated with morphological features related to light competition and plant height (43–45). Yet, similarly to our results, the dominant axes of physiological and morphological plant features did not strongly covary across latitudinal gradients (44, 45). Together, our findings and previous research suggest that organismal function that supports rapid growth is not necessarily linked to organismal function that results in lower life expectancies and small maximal sizes. These emergent patterns suggest that rapid shifts in climate conditions may have divergent effects on the relationship between biomass accumulation in tree

growth and biomass retention in tree longevity, with important implications for modeling the global carbon balance in a changing world (46).

Demographic diversity varies predictably across biogeographic gradients (H3)

To characterize the range of life history strategies that are expressed by trees across broad-scale biogeographic gradients, we first calculated the convex-hull volume in demographic trait space within each grid cell (SM, materials and methods) (47) and compared the relationship between the demographic trait diversity of forests and well-established patterns in species richness. The convex-hull volume was calculated by using the life history trait PC scores for axes 1 to 3, which together captured 95% of the life history trait variation. We then tested whether the demographic trait diversity of forests varied predictably across biogeographic gradients and explored potential links between demographic trait diversity and remotely sensed estimates of potential aboveground net primary productivity (NPP) (Fig. 1C, H3, and SM, materials and methods) (48). The expectation is that the diversity of life history trait strategies that are expressed by trees should vary predictably across biogeographic gradients, with higher demographic diversity being positively associated with aboveground productivity.

Our results illustrate that the demographic trait diversity of forests follows well-established patterns in species richness [Fig. 4A, adjusted coefficient of determination ($\text{adj } R^2$) = 0.65, $P < 0.001$]. We also found that the demographic diversity of forests varied predictably across biogeographic gradients, with high demographic trait diversity across warm tropical forests and low diversity of predominantly slow-growing, long-lived species in the cold temperate and boreal forests ($\text{adj } R^2$ = 0.40, $P < 0.001$; Fig. 4B and table S7). Lastly, we found a positive correlation between the demographic diversity of forests and remotely sensed estimates of ecosystem productivity (Pearson's r = 0.71).

The emergence of a positive association between the demographic trait diversity and ecosystem productivity is in line with two non-mutually exclusive hypotheses. From an evolutionary perspective, ecosystem productivity is thought to drive species diversification and niche differentiation (49). Conversely, following widely established relationships between biodiversity and ecosystem function, more demographically diverse forests are commonly assumed to have access to a larger resource pool and should thus be more productive (50, 51). In this study, we found moderate support for both hypotheses. Specifically, we found that ecosystem productivity was predictive of demographic trait diversity across broadscale biogeographic gradients ($\text{adj } R^2$ = 0.49, $P <$

0.001; Fig. 4C and table S7). At the same time, ecosystem productivity was jointly influenced by temperature (average marginal effect = 0.83, P = 0.04; Fig. 4D) and demographic trait diversity (average marginal effect = 1.43, $P < 0.001$; Fig. 4D). This positive association was consistent across the tropics ($\text{adj } R^2$ = 0.26, $P < 0.01$; table S7) and extra-tropics ($\text{adj } R^2$ = 0.84, $P < 0.01$; Fig. 4D and table S7). It should be noted that NPP was strongly correlated with mean annual temperature (Pearson's r = 0.94), which did not allow us to explicitly test for the individual and combined effect of these variables on demographic trait diversity. Although our broadscale analysis does not establish causality in the direction of these relationships, it does highlight the inextricable link between demographic trait diversity and ecosystem productivity across forest biomes.

The established association between demographic trait diversity and ecosystem productivity is in line with emergent patterns derived from tropical forest plots, which found that the demographic composition of forests was predictive of empirically derived measures of aboveground carbon dynamics (32). Similarly, our findings match theoretical expectations that the pace of life of organisms within a community (e.g., life expectancy and generation time) should strongly regulate the relationship between carbon turnover (ecosystem fluxes) and carbon retention (ecosystem pools) (52). It is important to note that the association between demographic trait diversity and ecosystem productivity was derived from multiyear averages in remotely sensed NPP from 1997 to 2013 and from mean estimates of tree growth–longevity–stature relationships that were based on the current distribution of species (i.e., derived from dynamical data collected from the 1900s to 2000s). This approach did not allow us to account for potential biogeographic biases in the effects of human disturbance on species diversity (i.e., between boreal and tropical forests). Yet, by quantifying the current distribution of demographic functional types across broadscale resource gradients, our results provide a powerful backdrop for parameterizing next-generation vegetation models to simulate forest carbon turnover rates across a range of current and future conditions.

More generally, our analysis offers strong empirical support for the expectation of high demographic trait diversity in tropical forests as compared with temperate and boreal forests. This multibiome finding supports the community assembly theory of strong abiotic filtering in boreal regions, which results in a restricted species pool of predominantly slow-growing, long-lived species (Fig. 1C, H3). This emergent pattern is congruent with known variability in physiological leaf trait characteristics across biogeographic gradients (43–45), with decreasing variation in leaf economic traits from lower

to higher latitudes (53). Similarly, our results match well-established species richness–productivity relationships across global forests (51, 54) and community structure–productivity relationships (55). Yet, although it makes intuitive sense that the demographic diversity of forest communities follows well-established patterns in species richness (49, 50), our findings establish a more direct link to the demographic mechanisms that generate global variation in ecosystem carbon turnover.

Conclusions

Our broadscale analysis reveals the remarkable diversity of life history strategies that exist for tree species across the Americas. Weak trade-offs between tree growth, longevity, and stature across biogeographic gradients demonstrate the modular and flexible nature of trees, highlighting the diversity of evolutionary trajectories that have arisen to address the ecological puzzle of survival. In addition, from a functional perspective, we found that although acquisitive trees sequester carbon at faster rates, they also generally appear constrained to smaller maximum sizes and shorter life spans that translate to lower carbon storage and faster carbon turnover. More importantly, we found that more demographically diverse forests tend to be more productive at the ecosystem scale across the tropics and extratropics. These findings have important implications for informing global restoration and conservation efforts and for understanding the fundamental feedback between biodiversity and climate change mitigation.

REFERENCES AND NOTES

1. H. Caswell, *Matrix Population Models*, vol. 1 (Sinauer, 2000).
2. C. J. E. Metcalf, C. C. Horvitz, S. Tuljapourkar, D. A. Clark, *Ecology* **90**, 2766–2778 (2009).
3. J. P. de Magalhães, J. Costa, G. M. Church, J. Gerontol. A Biol. Sci. Med. Sci. **62**, 149–160 (2007).
4. D. E. L. Promislow, *J. Gerontol.* **48**, B115–B123 (1993).
5. S. C. Stearns, *Funct. Ecol.* **3**, 259 (1989).
6. N. G. McDowell et al., *Science* **368**, eaaz9463 (2020).
7. U. Büntgen et al., *Nat. Commun.* **10**, 2171 (2019).
8. C. Körner, *Science* **355**, 130–131 (2017).
9. P. B. Reich, *J. Ecol.* **102**, 275–301 (2014).
10. S. E. Russo et al., *Nat. Ecol. Evol.* **5**, 174–183 (2021).
11. R. Salguero-Gómez et al., *Proc. Natl. Acad. Sci. U.S.A.* **113**, 230–235 (2016).
12. G. M. Locosselli et al., *Proc. Natl. Acad. Sci. U.S.A.* **117**, 33358–33364 (2020).
13. D. A. Clark, D. B. Clark, *Ecol. Appl.* **9**, 981–997 (1999).
14. R. J. W. Brien et al., *Nat. Commun.* **11**, 4241 (2020).
15. M. E. Cochran, S. Ellner, Simple Methods for Calculating Age-Based Life History Parameters for Stage-Structured Populations, Figshare (2016); <https://doi.org/10.6084/m9.figshare.c.3308904.v1>.
16. S. Tuljapourkar, C. C. Horvitz, *Ecology* **87**, 1497–1509 (2006).
17. C. C. Horvitz, S. Tuljapourkar, *Am. Nat.* **172**, 203–215 (2008).
18. ForestPlots.net, *Biol. Conserv.* **260**, 108849 (2021).
19. G. Lopez-Gonzalez, S. L. Lewis, M. Burkhitt, O. L. Phillips, *J. Veg. Sci.* **22**, 610–613 (2011).
20. R. Condit, *Tropical Forest Census Plots* (Springer-Verlag, 1998).
21. R. Condit et al., Complete data from the Barro Colorado 50-ha plot: 423617 trees, 35 years, version 3, Dryad (2019); <https://doi.org/10.15146/5XCP-0D46>.

22. J. K. Zimmerman, L. S. Comita, J. Thompson, M. Uriarte, N. Brokaw, *Landsc. Ecol.* **25**, 1099–1111 (2010).
23. "The Forest Inventory and Analysis Database: Database Description and User Guide for Phase 2 (version 9.1)," (Forest Service, US Department of Agriculture, 2024); <https://usfs-public.app.box.com/v/FIA-FIADB-UserGuides/file/1537460550704>.
24. Forest Analysis and Inventory Branch, "Forest Inventory Ground Plot Data and Interactive Map," British Columbia Data Catalogue (2023); <https://catalogue.data.gov.bc.ca/dataset/824e684b-4114-4a05-a490-aa56332b57f4>.
25. Ministry of Forests, Wildlife and Parks, "Networks of Permanent Sample Plots in Southern Quebec" (in French) (Government of Quebec, Ministry of Forests, Wildlife and Parks, Forest Inventories Directorate, 2014); <https://mfp.gouv.qc.ca/documents/forets/inventaire/Reseaux-PEP.pdf>.
26. M. R. Easterling, S. P. Ellner, P. M. Dixon, *Ecology* **81**, 694–708 (2000).
27. P. A. Zuidema, E. Jongejans, P. D. Chien, H. J. During, F. Schieving, *J. Ecol.* **98**, 345–355 (2010).
28. G. Kunstler et al., *J. Ecol.* **109**, 1041–1054 (2021).
29. S. Ellner, D. Z. Childs, M. Rees, *Data-Driven Modelling of Structured Populations* (Springer International, 2016).
30. G. Piovesan, F. Biondi, *New Phytol.* **231**, 1318–1337 (2021).
31. N. Rüger et al., *Science* **368**, 165–168 (2020).
32. J. F. Needham et al., *Glob. Change Biol.* **28**, 2895–2909 (2022).
33. S. Kambach et al., *J. Ecol.* **110**, 1485–1496 (2022).
34. N. Rüger et al., *Ecol. Lett.* **21**, 1075–1084 (2018).
35. A. Esquivel-Muelbert et al., *Nat. Commun.* **11**, 5515 (2020).
36. S. J. Wright et al., *Ecology* **91**, 3664–3674 (2010).
37. L. Poorter et al., *Ecology* **89**, 1908–1920 (2008).
38. D. M. A. Rozendaal, R. J. W. Brienens, C. C. Soliz-Gamboa, P. A. Zuidema, *New Phytol.* **185**, 759–769 (2010).
39. J. D. Hadfield, *J. Stat. Softw.* **33**, 1–22 (2010).
40. J. D. Hadfield, S. Nakagawa, *J. Evol. Biol.* **23**, 494–508 (2010).
41. F. Coelho de Souza et al., *Proc. Biol. Sci.* **283**, 20161587 (2016).
42. B. Halliwell, B. R. Holland, L. A. Yates, Multi-Response Phylogenetic Mixed Models: Concepts and Application. *bioRxiv* 2022.12.13.520338 [Preprint] (2022). <https://doi.org/10.1101/2022.12.13.520338>.
43. S. Díaz et al., *Nature* **529**, 167–171 (2016).
44. J. S. Joswig et al., *Nat. Ecol. Evol.* **6**, 36–50 (2022).
45. D. S. Maynard et al., *Nat. Commun.* **13**, 3185 (2022).
46. N. Carvalhais et al., *Nature* **514**, 213–217 (2014).
47. W. K. Cornwell, L. D. Schwillk, D. D. Ackerly, *Ecology* **87**, 1465–1471 (2006).
48. S. E. Fick, R. J. Hijmans, *Int. J. Climatol.* **37**, 4302–4315 (2017).
49. David Tilman, *Resource Competition and Community Structure*. Princeton University Press, 1982 (Princeton Univ. Press, 1982).
50. D. Tilman et al., *Science* **277**, 1300–1302 (1997).
51. J. Liang et al., *Science* **354**, aaf8957 (2016).
52. M. Sobral, M. Schleuning, A. Martínez Cortizas, *Trends Ecol. Evol.* **38**, 602–604 (2023).
53. E. E. Butler et al., *Proc. Natl. Acad. Sci. U.S.A.* **114**, E10937–E10946 (2017).
54. H. Hillebrand, *Am. Nat.* **163**, 192–211 (2004).
55. T. I. Kohyama et al., *Nat. Commun.* **14**, 1113 (2023).
56. L. Bialic-Murphy, R. McElerry, The pace of life for forest trees, Zenodo (2024); <https://doi.org/10.5281/zenodo.11615767>.

ACKNOWLEDGMENTS

We thank the international team of network collaborators, including those who are not coauthors on this paper, for sharing their valuable plot datasets and providing their insights and support for this project. This study was enabled by the Global Forest Dynamics database, initiated by the TreeMort project, on which this study is based. The tropical tree analyses were enabled by the ForestPlots.net research project no. 169 ("Placing life history trait variation of forest trees in an evolutionary and environmental context"). ForestPlots.net is a global collaboration and meta-network supported from the University of Leeds (18, 19). **Funding:** T.A.M.P., A.E.-M., and O.L.P. acknowledge support from the European Research Council (ERC) under the European Union's Horizon 2020 research and innovation program (grant agreement 758873, TreeMort). A.E.-M. was further funded by the Royal Society Standard Grant RGS\R1\221115 "MegaFlora," the UKRI/NERC TreeScapes NE/V021346/1 "MEMBRA," the NERC/NSF Gigante NE/V003942/1, and the FRB/CESAB "Syntreesys." O.L.P. and ForestPlots.net data management have been supported by several grants, including from the UK Natural Environment Research Council ("AMSINK" NE/X014347/1, "SECO" NE/T012722/1, "BIO-RED" NE/N012542/1, and "ARBOLES" NE/S011811/1), as well as from the European Research Council, the European Space Agency, the European Union, and the Royal Society. ForestPlots.net partners acknowledge many additional sources of funding: Instituto Nacional de Ciência e Tecnologia (INCT) grant 465610/2014-5, FAPESP grant 2018/0267000023, the Brazilian National Council for Scientific and Technological Development (CNPq) (PELD CNPq grant 403710/2012-0 and CNPq/Universal grant 459941/2014-3), the British Natural Environment Research Council/NERC (NE/K016431/1), and FAPESP (BIOTA grants 2003/12595-7, 2012/51509-8, and 2012/51872-5); doctoral and postdoctoral fellowships from FAPESP (FAPESP 11/11604-0 and 22/09041-0); Project Sustainable Landscapes (US Forest Service, USAID, EMBRAPA, and NASA-Goddard); CNPq (PELD-TRAN 441244/2016-5 and 441572/2020-0); Mato Grosso State Research Support Foundation (FAPEMAT) (grant 0346321/202); the NERC Knowledge Exchange Fellowship (grant NE/V018760/1); NERC Amazon Past Fire Project (NE/N011570/1), CAPES Project (PVE177-2012), CNPq grants 441282/2016-4, 403764/2012-2, and 558244/2009-2 for IFA LTER plots; FAPEAM grants 1600/2006, 465/2010, and PPFOR 147/2015; and CNPq grants 473308/2009-6 and 558320/2009-0, which funded the monitoring of Purus-Madeira interfluvium. The BCI forest dynamics research project was made possible by NSF grants to S. P. Hubbell: DEB-0640386, DEB-0425651, DEB-0346488, DEB-0129874, DEB-00753102, DEB-9909347, DEB-9615226, DEB-9615226, DEB-9405933, DEB-9221033, DEB-9100058, DEB-8906869, DEB-8605042, DEB-8206992, and DEB-7922197; through support from the Forest Global Earth Observatory (ForestGEO), the Smithsonian Tropical Research Institute, the John D. and Catherine T. MacArthur Foundation, the Mellon Foundation, the Small World Institute Fund, and numerous

private individuals; and through the hard work of over 100 people from 10 countries over the past three decades. Research at the Wabikon Forest Dynamics Plot was supported by the 1923 Fund, the Cofrin Center for Biodiversity at the University of Wisconsin–Green Bay, and the US Forest Service. The Luquillo ForestGeo dataset was supported by grants BSR-8811902, DEB 9411973, DEB 0080538, DEB 0218039, DEB 0620910, DEB 0963447, and DEB-129764 from NSF to the Department of Environmental Science, University of Puerto Rico, and to the International Institute of Tropical Forestry, USDA Forest Service, as part of the Luquillo Long-Term Ecological Research Program. The US Forest Service (Department of Agriculture) and the University of Puerto Rico gave additional support. The BIC, Luquillo, and Wabikon plots were part of the Smithsonian Institution Forest Global Earth Observatory, a worldwide network of large, long-term forest dynamics plots. T.A.M.P. and J.A. acknowledge funding from the CLIMB-FOREST Horizon Europe Project (no. 101059888) that was funded by the European Union. G.D. acknowledges support from an "Investissement d'Avenir" grant managed by Agence Nationale de la Recherche (CEBA, ref. ANR-10-LABX-25-01). **Author contributions:** L.B.-M. led the writing of this manuscript, with substantial input from T.W.C., R.M.M., A.E.-M., J.v.d.H., P.A.Z., and T.A.M.P. L.B.-M. led the analysis, with input from R.M.M. and P.A.Z. A.E.-M., T.A.M.P., O.L.P., J.A., K.M.B., and L.B.-M. assembled and integrated the tree dynamics database, with contributions from other ForestPlots.net and TreeMort network partners. All authors collected and curated data from inventory plots, provided feedback on the results, and contributed to the writing of the manuscript. **Competing interests:** The authors declare that they have no competing interests. **Data and materials availability:** The plot-level input data and R code that are needed to replicate our analyses are available at https://github.com/Lalasia/pace_of_life/ and Zenodo (56). The tree-by-tree observations used to generate the plot-level input data are also published with this paper. However, this file does not include data from networks with sensitive species or a need for indigenous data sovereignty. These data are available upon request for research purposes by emailing the following networks: Alberta Agriculture and Forestry Division <https://www.alberta.ca/permanent-sample-plots-program>, email: af.fm-biometrics@gov.ab.ca, Saskatchewan Minister of Environment Forest Service Branch <https://www.saskatchewan.ca/contact-us>, ForestGeo <https://forestgeo.si.edu/explore-data> (20–22), and ForestPlots.net <https://forestplots.net/en/using-forestplots/in-the-field>, email: admin@forestplots.net (18, 19). **License information:** Copyright © 2024 the authors, some rights reserved; exclusive licensee American Association for the Advancement of Science. No claim to original US government works. <https://www.science.org/about/science-licenses-journal-article-reuse>

SUPPLEMENTARY MATERIALS

science.org/doi/10.1126/science.adk9616
Materials and Methods
Figs. S1 to S15
Tables S1 to S7
References (57–68)

Submitted 28 October 2023; accepted 28 August 2024
[10.1126/science.adk9616](https://doi.org/10.1126/science.adk9616)

Correction (18 October 2024): Several errors regarding author affiliations and roles were introduced in the online version of this article during the publication process and have now been corrected. The print edition and downloadable pdf required minimal correction.